International Journal of Modern Physics C
Vol. 18, No. 4 (2007) 644–651

World Scientific
www.worldscientific.com

EFFECTS OF ATOMISTIC DOMAIN SIZE ON HYBRID LATTICE BOLTZMANN—MOLECULAR DYNAMICS SIMULATIONS OF DENSE FLUIDS

A. DUPUIS* and P. KOUMOUTSAKOS†

Computational Science and Engineering Laboratory
ETH Zurich, CH-8092, Switzerland
**dupuisa@inf.ethz.ch*
†petros@ethz.ch

We present a convergence study for a hybrid Lattice Boltzmann-Molecular Dynamics model for the simulation of dense liquids. Time and length scales are decoupled by using an iterative Schwarz domain decomposition algorithm. The velocity field from the atomistic domain is introduced as forcing terms to the Lattice Boltzmann model of the continuum while the mean field of the continuum imposes mean field conditions for the atomistic domain. In the present paper we investigate the effect of varying the size of the atomistic subdomain in simulations of two dimensional flows of liquid argon past carbon nanotubes and assess the efficiency of the method.

Keywords: Lattice Boltzmann model; Molecular Dynamics; nanofluidics; multiscale.

PACS Nos.: 67.55.Hc, 61.46.Fg, 61.20.Ja, 68.65.-k.

1. Introduction

The modeling of nanoscale systems such as biosensors and actuators [1] operating in a macroscale environment requires a multiscale modeling approach. A particular challenge involves the modeling and simulation of devices embedded in an aqueous environment when considering biological applications.

Molecular Dynamics (MD) simulate nanoscale systems by modeling the interactions between atoms. State-of-the-art MD have been used to simulate systems that can be described with up to a few millions atoms for a few nanoseconds. Nanoscale devices are often part of microscale applications making MD simulations of the complete system prohibitive. In turn modeling of these systems requires the design of hybrid approaches capable of integrating atomistic simulations with computational methods suitable for simulations of continuum systems.

Several hybrid models coupling atomistic to continuum descriptions of dense fluids have been proposed [2]. In particular, Werder *et al.* [3] designed an algorithm using the alternating Schwarz method to couple an MD model to an incompressible Navier-Stokes (NS) Finite Volume solver. They proposed a novel boundary force, based on the physical characteristics of the fluid that is being simulated. They

reported on simulations of flows past a carbon nanotube (CNT) and noticed average departures from reference MD simulations of the order of 4%.

We have recently extended [4] Werder's work to hybrid models where the Lattice Boltzmann (LB) method [5] is used to simulate the incompressible NS equations. We have shown good quantitative agreement between hybrid results and reference MD solutions for flows of liquid argon past and through CNTs.

The efficiency of the proposed MD-LB model is controlled by the the size of the atomistic region. The larger the atomistic domain the poorer the computational efficiency. At the same time large atomistic domains enable a better sampling and in turn a better match with the reference solution. The aim of this paper is to assess this trade-off by quantifying the effect of the size of the atomistic domain on the convergence of the method.

The paper is organized as follows. In section 2, we describe the hybrid model by presenting MD and LB numerical methods as well as their coupling. Results of argon flows past a CNT are presented in section 3. We compare hybrid flows to the reference MD solutions and discuss the computational efficiency of the hybrid model before concluding in section 4.

2. The LB-MD model

2.1. *Molecular Dynamics (MD)*

The atomistic region is described by classical MD simulations where the positions $\mathbf{r}_i = (x_i, y_i, z_i)$ and velocities $\mathbf{u}_i = (u_{x,i}, u_{y,i}, u_{z,i})$ of the particles evolve according to Newton's equations of motion

$$\frac{d}{dt}\mathbf{r}_i = \mathbf{u}_i \quad \text{and} \quad m_i \frac{d}{dt}\mathbf{u}_i = \mathbf{F}_i = -\sum_{j \neq i} \nabla U(r_{ij}) \tag{1}$$

where $\mathbf{F}_i$ and m_i are the force and mass of particle i, and r_{ij} is the distance between the particle $\mathbf{r}_i$ and $\mathbf{r}_j$. Here we consider Lennard-Jones (LJ) argon interacting with CNTs. The LJ interaction parameters for argon-argon and argon-carbon interactions are respectively $\epsilon_{ArAr} = 0.9960$ kJmol^{-1}, $\sigma_{ArAr} = 0.3405$ nm, $\epsilon_{ArC} = 0.5697$ kJmol^{-1}, $\sigma_{ArC} = 0.3395$ nm. The CNT is modeled as a rigid structure. The equations of motion (1) are integrated using a leap-frog scheme with a time step of $\delta t = 10$ fs.

The MD system is influenced by the continuum system through the imposition of a mean velocity $\mathbf{u}_d$ at each cell. The mean velocity is enforced by relaxing the center of mass velocity $\bar{\mathbf{u}}_k = 1/N_k \sum_{i \in k} \mathbf{u}_i$ of the N_k particles within a cell k towards $\mathbf{u}_d$[4]. In turn the atomistic system is sampled in order to provide a velocity field as boundary conditions for the LB solver.

2.2. *Lattice Boltzmann (LB) model of the Navier-Stokes equations*

The atomistic domain is coupled to a domain of continuum hydrodynamics described by the incompressible Navier-Stokes equations

$$\frac{\partial \mathbf{u}}{\partial t} + (\mathbf{u} \cdot \nabla)\mathbf{u} = -\nabla p/\rho + \nu \nabla^2 \mathbf{u} + \mathbf{g}, \tag{2}$$

$$\nabla \cdot \mathbf{u} = 0. \tag{3}$$

Here $\mathbf{u}$ denotes the fluid velocity, p the pressure, ρ the density and $\mathbf{g}$ a body force. We use $\mathbf{g}$ to enforce Dirichlet boundary conditions, see discussion below.

The equations of motion (2) and (3) are solved using a Lattice Boltzmann algorithm [5]. This approach follows the evolution of particle distribution functions f_i on a d-dimensional regular lattice with z links at each lattice point $\mathbf{r}$. The label i denotes velocity directions and runs between 0 and z. $DdQz+1$ is a standard lattice topology classification. The $D3Q15$ lattice we use here has the following velocity vectors $\mathbf{v}_i$: $(0,0,0)$, $(\pm1,\pm1,\pm1)$, $(\pm1,0,0)$, $(0,\pm1,0)$, $(0,0,\pm1)$ in lattice units. The LB dynamics are given by

$$f_i(\mathbf{r} + \Delta t \mathbf{v}_i, t + \Delta t) = f_i(\mathbf{r}, t) + \frac{1}{\tau}\left(f_i^{eq}(\mathbf{r}, t) - f_i(\mathbf{r}, t)\right) + \Delta t g_i \tag{4}$$

where Δt is the time step of the simulation, τ the relaxation time. f_i^{eq} is the equilibrium distribution function which is a function of the density ρ and the fluid velocity $\mathbf{u}$, defined through the relations

$$\rho = \sum_{i=0}^{z} f_i \quad , \quad \rho \mathbf{u} = \sum_{i=0}^{z} f_i \mathbf{v}_i + \frac{\Delta t}{2}\mathbf{g}. \tag{5}$$

The equilibrium distribution function is chosen as

$$f_i^{eq}(\mathbf{r}, t) = w_i \rho \left(1 + \frac{\mathbf{v}_i \cdot \mathbf{u}}{c_s^2} + \frac{(\mathbf{v}_i \cdot \mathbf{u})^2}{2c_s^4} - \frac{\mathbf{u}^2}{2c_s^2}\right) \tag{6}$$

where $c_s = 1/\sqrt{3}$ is the speed of sound and w_i are weights chosen as $w_0 = 4/9$, $w_i = 1/9$ for $i = 1-6$ and $w_i = 1/72$ for $i = 7-14$. The forcing term is defined as [6]

$$g_i = \left(1 - \frac{1}{2\tau}\right) w_i \rho \left(\frac{\mathbf{v}_i - \mathbf{u}_i}{c_s^2} + \frac{(\mathbf{v}_i \cdot \mathbf{u}_i)}{c_s^4}\mathbf{v}_i\right) \cdot \mathbf{g}. \tag{7}$$

Performing a Chapman-Enskog multiscale expansion on the LB dynamics [7] shows that equations (2) and (3) are recovered in the low Mach number limit.

We enforce Dirichlet boundary conditions using a local forcing term $\mathbf{g}$ expressed as

$$\mathbf{g}(\mathbf{r}, t) = \frac{\mathbf{u}^d(\mathbf{r}, t + \Delta t) - \mathbf{u}^*(\mathbf{r}, t + \Delta t)}{\Delta t} \tag{8}$$

where $\mathbf{u}^*$ is the velocity at time $t + \Delta t$ with no forcing term considered and $\mathbf{u}^d$ is the desired velocity. More detail can be found in [4].

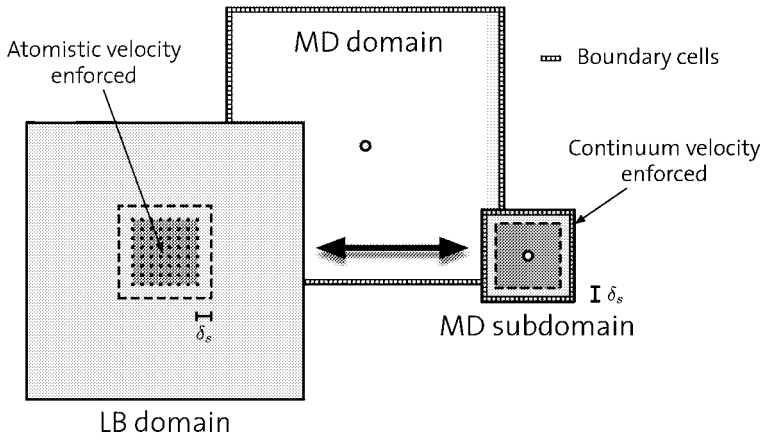

Fig. 1. Domain decomposition into an LB domain and an MD subdomain. Converged solution is obtained by alternating iterations in the domains. The dark gray area is computed within the MD subdomain and enforced within the LB domain whereas LB (continuum) velocities are used as outer boundary conditions within the MD subdomain.

2.3. *Hybrid model*

We use a domain decomposition algorithm to couple an MD description of a dense fluid with an LB model solving the incompressible NS equations. The computational domain consists of two overlapping regions: an LB domain covering the entire domain and an MD subdomain. Fig. 1 shows the Schwarz decomposition used to converge to a steady state solution by alternating iterations between steady state solutions in the LB domain and MD subdomain. A Schwarz cycle t_c consists of computing the continuum velocity field $\mathbf{u}_c(t_c)$ with boundary conditions set by the previous atomistic cycle $\mathbf{u}_a(t_c-1)$ and an external boundary condition that depends on the system considered. Then, $\mathbf{u}_c(t_c)$ is used to set the boundary condition for computing $\mathbf{u}_a(t_c)$.

The exchange of information between the domains are as follows. MD velocities are sampled in cells of same size as in the LB domain. They are enforced using equation (8) on every common cell except within a strip of width δ_s close to the boundary, see fig. 1. Enforcing velocities within a region results also in imposing velocity gradients and has been shown [4] to lead to hybrid results closer to the reference solution as compared to enforcing velocities along a strip. To impose non-periodic boundary conditions on the MD system we use the algorithm proposed by Werder *et al.* [3].

3. Results

We apply the hybrid LB-MD algorithm to the case of the flow of argon around a CNT centered along the z-axis within a $30 \times 30 \times 4.254$ nm^3 domain Ω. The CNT is of $(16, 0)$ chirality with a radius of $r = 0.625$ nm. We choose the density

of argon $\rho_{Ar} = 1008$ kgm^{-3} and the temperature $T = 215$ K. This corresponds to the dimensionless state point $(T^*, \rho^*) = (1.8, 0.6)$ where $T^* = k_B T \epsilon_{ArAr}^{-1} \mathcal{A}$ and $\rho^* = \rho \sigma_{ArAr}^3 m_{Ar}^{-1} \mathcal{A}$. We let k_B be the Boltzmann constant, $m_{Ar} = 0.03994$ kgmol^{-1} the atomic mass of argon, and $\mathcal{A}$ Avogadro's number.

The MD subdomain is centered around the CNT. We examine three different sizes of the atomistic subdomain in order to assess the effect of its size on the convergence of the hybrid approach. The sizes are $S_1 : 10 \times 10 \times 4.254$ nm^3, $S_2 : 6 \times 6 \times 4.254$ nm^3 and $S_3 : 4 \times 4 \times 4.254$ nm^3. MD subdomains are subdivided into sampling cells of size $0.5 \times 0.5 \times 4.254$ nm^3 where respectively $n_1 = 6465$, $n_2 = 2328$ and $n_3 = 1035$ argon atoms are initially equilibrated for 0.2 ns. The width of the strip around the boundary on which both MD and LB are simulated is $\delta_{1,2} = 2.5$ nm and $\delta_3 = 1.5$ nm.

We consider an LB domain of size $60 \times 60 \times 1$ covering the entire domain where lattice nodes are centered on the corresponding MD sampling cells. The relaxation time $\tau = 0.95$. The viscosity of the LJ fluid is a parameter of the LB model and set to $\nu = 0.745 \cdot 10^{-7}$ m^{2}s^{-1} [8]. We have performed a sensitivity analysis by increasing and decreasing the viscosity by 5% and found that it did not influence the accuracy of the method. Dirichlet boundary conditions $u_\infty = u_x = 100$ ms^{-1} are imposed at the inlet $x = 0$ nm and outlet $x = 30$ nm. This high velocity is chosen to reduce the number of sampling iterations. The temperature is controlled by using a Berendsen thermostat [9] with a time constant $\tau_T = 0.1$ ps. We apply the thermostat cell-wise in all directions in the boundary cells where the velocity is prescribed and only in the z-direction in other cells. The hybrid model is run for 100 cycles which consists of running the LB simulation for 7 ns (15000 iterations) followed by an MD step equilibrating for 0.2 ns (20000 iterations) and sampling for $t_s = 0.4$ ns. Considering shorter t_s leads to undesirable fluctuations whereas long t_s decreases the computational efficiency of the model. This is discussed in more detail in [4].

Fig. 2 shows hybrid converged solutions and an MD reference solution over the entire domain. The latter involves 58198 argon atoms and the temperature is controlled as in the MD subdomain. The reference MD velocity field is sampled over 20 ns. The hybrid solutions in fig. 2(a-c) and (d) agree quantitatively well over the entire domain. We observe however that the larger the MD subdomain the more accurate the hybrid result. The discrepancies in the wake and on the sides of the CNT reported in [3] are not observed here when a comparable size of the MD subdomain is considered, i.e. as in fig. 2(a).

We quantify the convergence of the method by defining an error e^j between the hybrid solution at cycle j and the reference MD solution as

$$e^j = \frac{1}{N} \sum_{k \in \Omega} \frac{|\mathbf{u}_k^j - \mathbf{u}_{k,MD}|}{u_\infty} \tag{9}$$

where N is the number of cells in Ω, $\mathbf{u}_k^j$ and $\mathbf{u}_{k,MD}$ are respectively the hybrid and reference MD velocities at cycle j in the cell k.

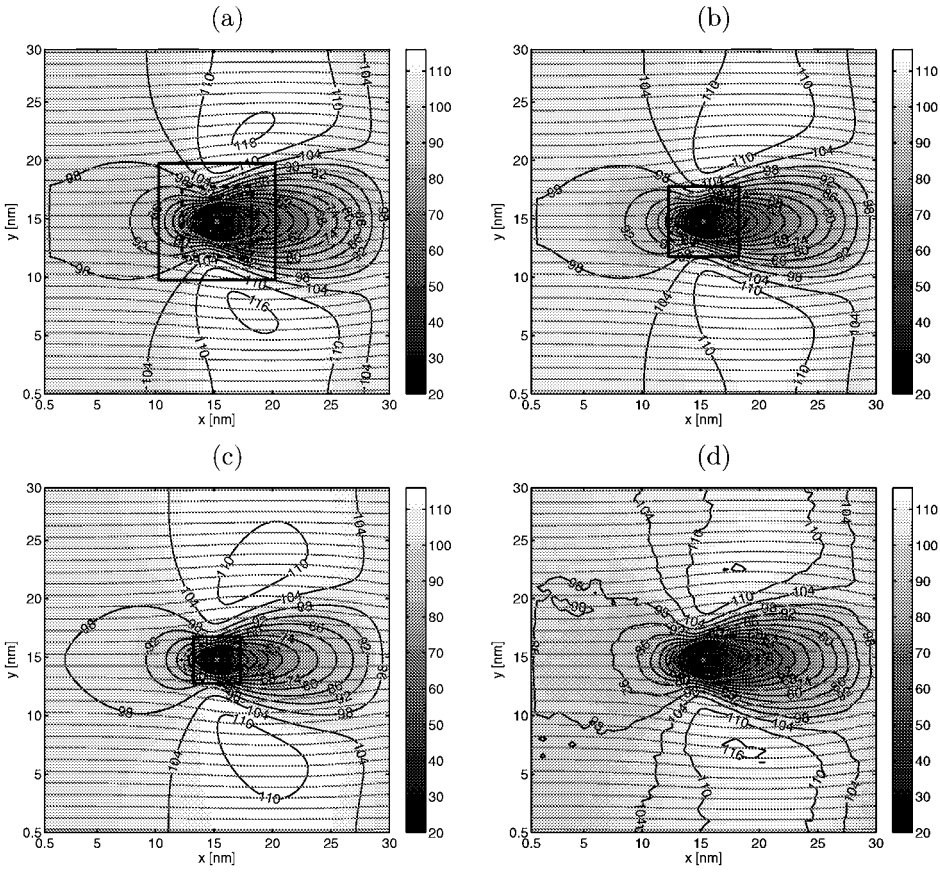

Fig. 2. (a-c) Converged hybrid and (d) reference MD solution of a flow past a CNT. MD subdomain sizes are (a) $10 \times 10 \times 4.254$ nm^3, (b) $6 \times 6 \times 4.254$ nm^3 and (c) $4 \times 4 \times 4.254$ nm^3. The colorscale and contour lines depict the norm of the velocity expressed in ms^{-1}. Gray lines are streamlines. Thick lines represent (solid) the boundary of the MD subdomain and (dashed) the boundary of the overlap region.

Fig. 3(a-c) shows a point-wise error between the hybrid solutions averaged between cycle 50 and 100, and the reference MD solution. A localized and maximum 3.9% error region shows in fig. 3(a) only on one side of the CNT. Everywhere else the error is up to 2.5%. Considering a smaller MD subdomain leads to larger error, see fig. 3(b,c). The flow close to the CNT shows the largest departure from the reference solution with errors up to (b) 12% and (c) 25%. We also observe departures in the wake and, especially when considering the smallest domain, on the side of the CNT.

Fig. 3(d) displays the time evolution of the error for the three sizes of the MD subdomains examined in this study. The error rapidly decays during the first 10 cycles. The error then fluctuates around an average value which is a function of

the MD subdomain size. We measure an average error between cycle 50 and 100 of $\langle e^j \rangle_1 = 1.3\%$, $\langle e^j \rangle_2 = 1.8\%$ and $\langle e^j \rangle_3 = 3.3\%$. We observe that the error curves plateau faster considering S_3, S_2 than S_1. This is due to the fact that simulation results fluctuate less for small domains than for large ones (considering a constant t_s) implying a faster convergence towards a steady state.

Fig. 3(d) also shows the time evolution of the error when the MD subdomain size is further extended to $12 \times 12 \times 4.254$ nm^3. The error plateaus at a later stage and reaches a value higher than the one obtained considering the domain of size S_1. This is because the sampling error due to t_s being constant becomes significant when S_4 is considered. Increasing t_s would improve the accuracy within S_4 but would not within S_1, see discussion in [4]. This indicates that given a t_s, there is an optimal size of the MD subdomain and that S_1 is a good approximation of it.

The computational efficiency of the LB-MD model is estimated by comparing the time needed to compute one iteration of the reference and hybrid solution, respectively. We measure $t_{ref} = 0.56$ s and $t_1 = 0.08$, $t_2 = 0.04$ and $t_3 = 0.03$ s implying that the hybrid solution is computed $R_1 = 0.56/0.08 = 7$, $R_2 = 14$ and $R_3 = 19$ times faster than the reference solution. Ratios R are of the same order as the volume ratio between the MD domain and subdomain. Small systems have been chosen here in order to compare hybrid to reference solutions. Considering larger systems would exhibit much higher ratios. For example, nanodevices ($\propto 10^3$ nm^3) embedded in microscale systems ($\propto 1$ μm^3) would lead to ratios of the order of 10^6.

4. Conclusion

We have examined the computational efficiency of a recently proposed hybrid model [4], coupling a Lattice Boltzmann description of the Navier-Stokes equations to Molecular Dynamics of liquids. The efficiency of the method was examined in terms of the size of the atomistic domain in hybrid simulations of liquid argon flow past a CNT.

We observed a good agreement between hybrid and reference MD solutions with an average error of $\langle e^j \rangle_1 = 1.3\%$, $\langle e^j \rangle_2 = 1.8\%$ and $\langle e^j \rangle_3 = 3.3\%$ depending on the size of the MD subdomain. These errors are the results of hybrid simulations computed $R_1 = 7$, $R_2 = 14$ and $R_3 = 19$ times faster than the reference solution with a constant sampling time t_s. Our results indicate a specific size of the MD subdomain that minimizes the average error $\langle e^j \rangle$.

References

1. N. Sinha, J. Ma, and J.T.W. Yeow. Carbon nanotube-based sensors. *J. Nanosci. Nanotechnol.*, 6, 2006.
2. P. Koumoutsakos. Multiscale flow simulations using particles. *Ann. Rev. Fluid Mech.*, 37:457, 2005.
3. T. Werder, J.H. Walther, and P. Koumoutsakos. Hybrid atomistic-continuum method for the simulation of dense fluid flows. *J. Comp. Phys.*, 205:373, 2005.

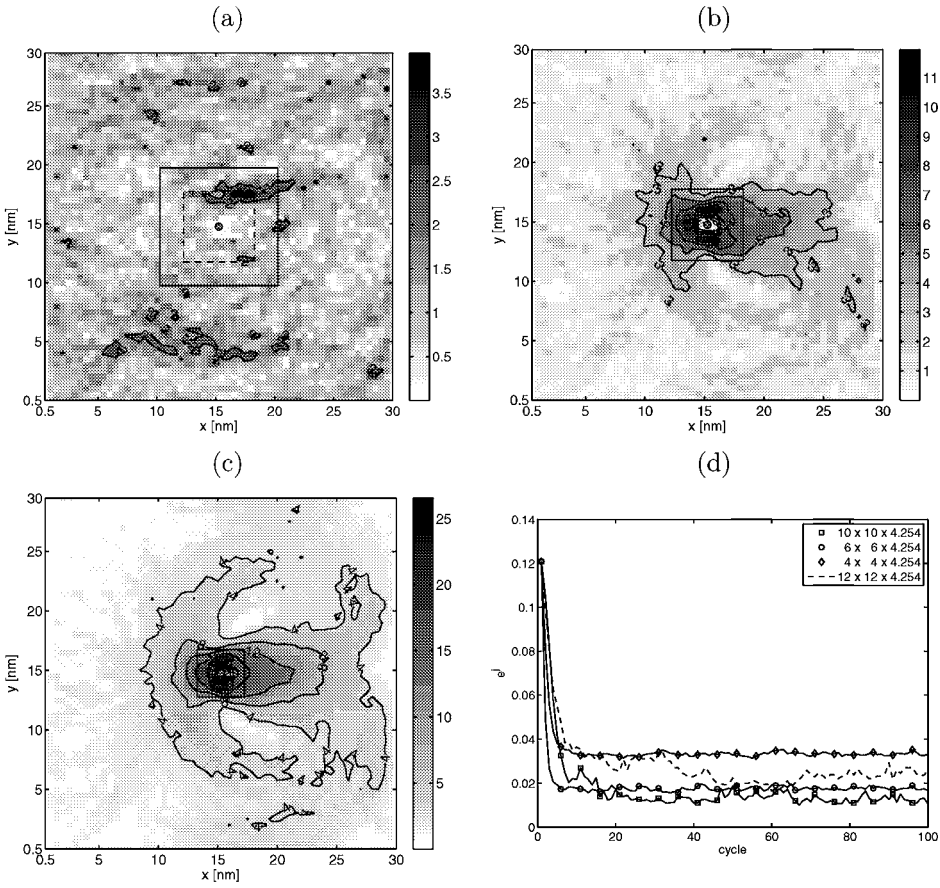

Fig. 3. (a-c) Point-wise error according to equation (9) shown in percentage and averaged between cycle 50 and 100. The squares show the boundary of the MD subdomain (a) $10 \times 10 \times 4.254$ nm^3, (b) $6 \times 6 \times 4.254$ nm^3 and (c) $4 \times 4 \times 4.254$ nm^3. (d) Evolution of the error e^j between the hybrid solutions (a-c) and the reference MD solution.

4. A. Dupuis, E.M. Kotsalis, and P. Koumoutsakos. Coupling Lattice Boltzmann and Molecular Dynamics models for dense fluids. *Submitted*, see /cond-mat/0610774.
5. S. Succi. *The Lattice Boltzmann Equation, For Fluid Dynamics and Beyond.* Oxford University Press, 2001.
6. Z. Guo, C. Zheng, and B. Shi. Discrete lattice effects on the forcing term in the lattice Boltzmann method. *Phys. Rev. E*, 65:046308, 2002.
7. B. Chopard and M. Droz. *Cellular Automata Modeling of Physical Systems.* Cambridge University Press, 1998.
8. K. Meier, A. Laesecke, and S. Kabelac. Transport coefficients of the Lennard-Jones model fluid. I. Viscosity. *J. Chem. Phys.*, 121:3671, 2004.
9. H.J.C. Berendsen, J.P.M. Postma, W.F. van Gunsteren, A. DiNola, and J.R. Haak. Molecular dynamics with coupling to an external bath. *J. Chem. Phys.*, 81:3684, 1984.